Noise Driven Transitions between Stable Equilibria in Stochastic Dynamical Systems

Kaitlin Daniels

May 12, 2011

Advised by Avanti Athreya and Jonathan Mattingly

1 Introduction

In this paper we examine two specific models of dynamical systems in which noise plays a central role. The first is a stochastic differential equation (SDE) modeling a particle in a potential well; the second is a simplified version of the Morris-Lecar model of a neuron. In each case, we consider both the underlying deterministic dynamical system, which is a governed by an ordinary differential equation, as well as the randomly-perturbed dynamical system, whose solution is a stochastic process satisfying a stochastic integral equation. We investigate the how perturbations of the drift functions influence transitions between stable equilibria and what effects such perturbations may have on exit times. We compare the results from computer simulations to analytical derivations of expected exit times. These results contribute to the understanding of the forces driving transitions between stable equilibria in perturbed dynamical systems.

2 Analytical Foundations

In this paper we focus on stochasic differential equations, particularly Ito integrals. We briefly recall the fundamentals of stochastic calculus, and refer to reader to the texts of Lawler [7] and Oksendal [9] for further details. Let $\Omega, \mathcal{F}, P$ represent our probability triple. We represent Standard Brownian Motion (SBM) by W_t, and note that W_t satisfies

1. $W_t \sim N(0,t)$
2. For all t,s, the increments $W_t - W_s$ are independent
3. With probability one, the trajectories W_t are continuous

While the total variation of Brownian motion is infinite, W_t has finite quadratic variation. That is to say, on any time interval $[0,t]$ and for any partition $[0 <= t_1 <= t_2 <= ... <= t]$,

$$E[(\Sigma_{t_k \in t}(\Delta W_{t_k})^2 - t)^2] \to 0 \tag{1}$$

as $\Delta t_k \to 0$.

The infinite total variation of Brownian motion renders it impossible to define a Riemann-Stieltjes integral with respect to the white noise process dW_t, but nevertheless the finite quadratic variation allows us to define an integral with respect to dW_t as a suitable L^2 limit. To be specific, let $\mathcal{F}_t$

represent the σ-algebra generated by W_t up to time t. Let $\mathcal{V}(T,P)$ represent the functions $f(t,\omega)$ which satisfy the following requirements:

1. For each t, ω, $f(t,w):[0,T]\to\mathbb{R}$ is measurable;
2. For each t, $f(t,w):\Omega\to\mathbb{R}$ is measurable with respect to $\mathcal{F}_t$;
3. $f(t,w)\in L^2\left([0,T]\times\Omega\right)$

It is possible to show (see Karatzas and Shreve [6]) that such functions can be approximated in L^2 by simple functions, i.e. functions of the form

$$S(t,w)=\sum_i^n e_i(w)1_{I_i}(t)$$

where 1_{I_i} is the indicator function of the time interval I_i. The Ito integral

$$\int_0^t f(s,w)dW_s$$

is first defined for these simple functions, and the Ito Isometry holds, namely:

$$E\left[\int_0^t S(t,w)dW_s\right]^2=E\left[\int_0^t S^2(s,w)ds\right]$$

Now, for any $f(t,w)\in\mathcal{V}$, there exists a sequence of simple functions $g_n\to f$ in $L^2\left([0,T]\times\Omega\right)$, and we can define

$$\int_0^t f(s,w)dW_s=\lim_{n\to\infty}\int_0^t g_n(s,w)dW_s$$

We note that Itô integrals are martingales.

We now introduce the process

$$dX_t=b(X_t)+\sigma dW_t \tag{2}$$

where σ is a fixed, positive constant and $b(X_t)$ is continuously differentiable. We intrepret the differential notation above as identifying a stochastic process X_t which satisfies the Itô integral equation

$$X_t=\int_0^t b(X_s)\mathrm{d}s+\int_0^t\sigma dW_s,\quad X_0=x \tag{3}$$

The existence and uniqueness of a solution X_t is guaranteed by Lipschitz continuity assumptions on the coefficients. Moreover, X_t is a continuous-time, real-valued Markov process, and as such we can define a transition operator associated to it. Specifically, we define the transition operator $\mathbf{T}_t f(x)$ as an operator which acts on real valued, bounded, Borel measurable functions, $\mathbf{T}_t f(x)$, such that

$$(\mathbf{T}_t f)(x) = E(f(X_t)|X_0 = x) = \int f(y)p(t; x, dy), \tag{4}$$

for $t > 0$ where $p(t; x, dy)$ is the transition probability of the Markov process X_t. We may then use this operator to introduce the infinitesimal generator $\mathbf{L}$ of X_t, defined by

$$(\mathbf{L}f)(x) = \lim_{s\to 0} \frac{(\mathbf{T}_s f)(x) - f(x)}{s}. \tag{5}$$

It can then be proven that, for any diffusion process on the interval (a, b) and any twice continuously differentiable f vanishing outside of a closed bounded subinterval,

$$(\mathbf{L}f)(x) = \mu(x)f'(x) + \frac{1}{2}\sigma^2 f''(x). \tag{6}$$

We refer the reader to Bhattachariya and Waymire [2] for a complete proof.

We observe that we can examine the behavior of X_t for varying values of σ. First, if the time interval $[0, T]$ is fixed, the behavior of $X_t = X_t^\sigma$ as $\sigma \to 0$ is governed by the solution to the deterministic system

$$\dot{x}_t = b(x_t), \quad x_0 = x,$$

in the sense that for any positive δ,

$$\lim_{\sigma\to 0} P\left(\sup_{0\le t\le T} |X_t^\sigma - x_t| > \delta\right) = 0,$$

so X_t^σ converges uniformly in probability on finite time intervals to x_t as $\sigma \to 0$. The proof of this may be found in the text of Freidlin-Wentzell [5].

On the other hand, if we consider exponentially long time intervals, i.e. $T \sim \exp(\lambda/\sigma)$ for some positive λ, then significant deviations between X_t^σ and x_t can occur even as $\sigma \to 0$, as described by the theory of large deviations (see [5] for a more detailed treatment). In this paper, however, we

consider fixed, moderate noise strength, so that transitions between stable equilibria and other noise-driven behavior in X_t can be readily observed and simulated.

In particular, we are interested in average escape times from stable equilibria. We denote the time of first exit from an interval as τ. We may now employ the Feynman-Kac formula to prove the following [7].

Claim. Consider a domain D and the following second order boundary value problem:

$$\mathbf{L}u(x) = -1 \tag{7}$$

$$u(x)\big|_{x\in\delta D} = 0 \tag{8}$$

for

$$\mathbf{L}u = b(x)\frac{du}{dx} + \frac{1}{2}\sigma^2\frac{d^2u}{dx^2} \tag{9}$$

Let $\tau = \inf\{t > 0 : X_t \in \delta D]\}$, the first time of exit domain D. Then $u(x) = E_x[\tau]$ is the unique solution to (1).

Proof: We apply Itô's to conclude

$$u(X_t) - u(x) = \int_0^t \{b(X_s)u'(X_s) + \frac{1}{2}\sigma^2 u''(X_s)\}\mathrm{d}s + \int_0^t \sigma \mathrm{d}X_s. \tag{10}$$

$$= \int_0^t \mathbf{L}u(X_s)\mathrm{d}s + \int_0^t \sigma \mathrm{d}W_s \tag{11}$$

from the definition of $\mathbf{L}$. Now, we let $\mathbf{L}u(X_s) = -1$ for $s \leq \tau$, yielding

$$u(X_\tau) - u(x) = \int_0^\tau -1\mathrm{d}s + \int_0^\tau \sigma \mathrm{d}W_s. \tag{12}$$

X_τ is assumed to be outside of the interval, so we apply the boundary condition $u(X_\tau) = 0$ to obtain

$$-u(x) = \tau + \int_0^\tau \sigma \mathrm{d}W_s. \tag{13}$$

Here we note that τ is a stopping time and that $E_z(\tau) < \infty$ because D is bounded and σ is fixed. We consider the expected value of (13).

$$E_z[-u(x)] = -E_z[\tau] + E[\int_0^\tau \sigma \mathrm{d}W_s] \tag{14}$$

whose left hand side is simply the deterministic expression $u(z)$. By the Optimal Stopping Theorem, $\int_0^\tau \sigma \mathrm{d}W_s$ is a martingale and so $E[\int_0^\tau \sigma \mathrm{d}W_s] = 0$. Thus $u(x) = E_x[\tau]$.

The infinitesimal generator and the Feynman-Kac formula establish a connection between the solutions to deterministic partial differential equations and solutions to stochastic differential equations which we will employ in analysis later in this paper.

3 Double Well Potentials

The first subject of our study is the double well potential. Double wells model systems composed of two attracting equilibria, much like two valleys between three hills. In a deterministic setting, a ball rolling along a hill between two valleys only reaches a new stable equilibrium when it has enough energy to overcome the hill in the middle. In physics, double wells are often used to describe the movement of a particle where each minimum represents a stable energy state. However, to accurately model the observed tunneling behavior of particles, the path of the particle is better described by a stochastic differential equation. Transitions between these stable equilibria would be impossible in a purely deterministic setting; indeed, they are a consequence of noise, and the time between transitions is a random variable. We can then ask questions about the distribution and expected value of transition times between stable equilibria.

We consider a particle whose motion is modeled by a double-well potential with additional deterministic oscillations. The new potential includes intermediate wells between the two absolute minima according to the period of a sinusoidal term. We examine not only the expected transition time between equilibria but also the effect of intermediate wells on the time to transition from one deepest well to the next. In this section we describe simulations of the motion of a particle within a double well with oscillatory terms and we investigate the effects of changes in period and amplitude in the oscillatory term. These simulations model double well systems with intermediate wells; also, we model systems from a "zoomed-in" perspective to compare the effects of adding a well to a double well potential and of changing the threshold level between wells in a simple triple well potential. The analytical results derived in this section demonstrate the isolated effects of additional wells and increased amplitude. Analytical evaluation of expected exit times for a stochastic process whose drift is a potential but with additional wells, each with small amplitude (i.e. depth of well), confirms that

amplitude influences transition times significantly.

3.1 Simulations

To create a double well potential with sinusoidal oscillations we add an oscillatory term to a standard expression a double well, yielding

$$V(x) = (x^2 - 1)^2 + a\cos(bx). \tag{15}$$

Motion within this well is defined according to

$$\mathrm{d}X_t = -V'(X_t)\mathrm{d}t + \mathrm{d}W_t \tag{16}$$

where σ represents noise strength, a represents the height of the threshold between intermediate wells, and b represents the period of the oscillations. Initial simulations set σ equal to a constant such that simulations generated sufficiently many transitions during a medium 25000 step run to consider the results of the run a valid sample. $V(x)$ has two deepest wells, one at $x = -1$ and the other at $x = 1$.

Our simulations concern transitions from one deepest well to the next while overcoming intermediate wells. σ is set to .7 and held constant. The trajectory representing particle motion within the system is generated according to the trapezoidal method outlined in Anderson and Mattingly [1]. To test the influence of a and b on transition times between deepest wells we run multiple simulations for varied values of parameters a, b, and σ. Values of b are limited to odd multiples of π to ensure that the system's deepest wells remain at $x = -1$ and $x = 1$ to produce data relevant for comparison with data from other runs. The time between each transition from deepest well to deepest well is fit to an exponential distribution. From this distribution we determine the expected value of the time between transitions under the given conditions. A mix of medium (approximately 25000 time steps) and long (250000 time steps) runs contribute to the reported average expected transition time for each set of parameter conditions.

3.2 Results

From our numerical exercises we glean that the path a particle takes along a potential well is significantly influenced by changes in the depth of the well but is unchanged by the number of intermediate wells added to the potential. While the existence of intermediate wells increases the expected transition time, the number of intermediate wells makes no significant difference. We

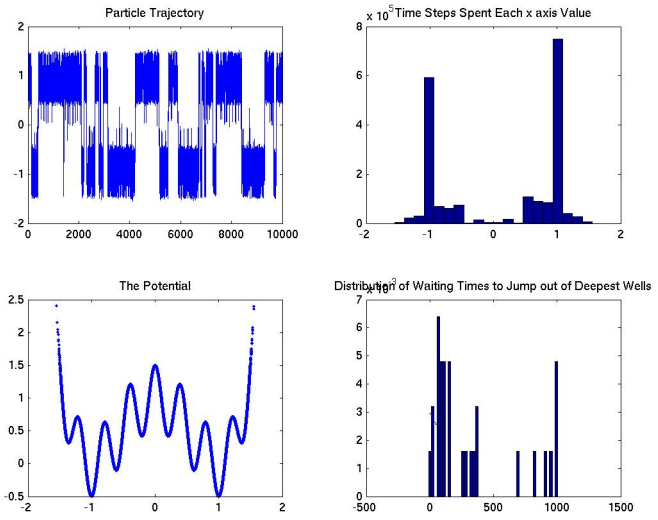

Figure 1: An example simulative output. Top left: a plot of the position X over time. Top right: a histogram tracking the proportion of time spent at each x location along the potential. Bottom right: the exponential fits of the recorded transition times generating a numerical value for expected transition time. Bottom left: a plot of the potential.

infer that the parameter a plays a significant role in transitions while b does not. The influence of a is expected. It stands to reason that taller thresholds between wells would inhibit transitions given our understanding of the behavior in deterministic well systems. Deeper wells require more energy from a deterministic particle to transition to the next well. Simulations demonstrate that higher thresholds have an analogous effect, strengthening the attractiveness of the stable equilibria and inhibiting transitions. The role of b is less intuitive. We hypothesize that the minimal effect of b on transition times is a result of the small amplitude of the intermediate wells relative to the amplitude of the double well without intermediate wells.

Ave Transition Time for Parameter Values				
σ	a	b	u_{ave}	perturbation
.7	0	11π	74	vary a
.7	.11	11π	90	
.7	.21	11π	124	
.7	.42	11π	198	
.7	.21	5π	93	vary b
.7	.21	7π	110	
.7	.21	9π	96	
.7	.21	11π	124	
.5	.21	11π	288	vary σ
.7	.21	11π	124	
1	.21	11π	11	

Table 1: Simulative results of perturbations of noise strength σ, amplitude of oscillations a, and number of intermediate wells b

3.3 Analytical Understanding

While these numerical results are telling, we are interested in analytical justifications so we may fully understand the behavior demonstrated by simulations. This section is devoted to the analysis and theoretical discussion of the double well problem.

In our case the diffusion process X_t is defined by the potential well curve and is of the form

$$\mathrm{d}X_t = b(X_t)\mathrm{d}t + \sigma \mathrm{d}W_t \tag{17}$$

where W_t is a standard Brownian motion. σ is a fixed parameter governing the strength of the noise, and the function $b(X_t)$ represents the negative derivative of the potential well function.

In Section 3.2 we established the uniqueness of the solution $u(x) = E_x[\tau]$ to the boundary problem $\mathbf{L} = -1$ and $u(x)\big|_x \in \delta D = 0$. We may now exploit this relationship to explicitly evaluate the expected time of first exit from a specified interval (c, d) along our potential wells. Starting from x, the expected time of first exit for the process X_t which is denoted $u(x)$, corresponds to the function $u(x)$ in the boundary value problem (7). From the Feynman Kac formula we obtain

$$-1 = b(x)u'(x) + \frac{1}{2}\sigma^2 u''(x). \tag{18}$$

Now we are presented with a second order linear differential equation. To solve we substitute $p(x) = u'(x)$ to reduce the expression to a first order ODE. Using the method of integrating factors we solve for $p(x)$

$$p(x) = \frac{\int_c^x \frac{-2}{\sigma^2} M(r)dr + K_1}{M(x)} \tag{19}$$

where $M(x) = exp^{\int_a^x \frac{2}{\sigma^2} b(z)dz}$ represents the integrating factor and K_1 is a constant of integration. To solve for $u(x)$ we simply integrate this expression to obtain

$$u(x) = \int_c^x \frac{\int_c^y \frac{-2}{\sigma^2} M(r)dr + K_1}{M(y)} \mathrm{d}y + K_2. \tag{20}$$

To solve for K_1 and K_2 we consider the boundary conditions. $u(x)$ represents the expected value of τ, the first exit from the interval (c, d) starting at x. Therefore, the expected value of τ for initial conditions outside of the interval is zero. We conclude that $u(c) = u(d) = 0$. Now we see that

$$0 = u(c) = \int_c^c \frac{\int_c^y \frac{-2}{\sigma^2} M(r)dr + K_1}{M(y)} \mathrm{d}y + K_2 \tag{21}$$

so $K_2 = 0$. We then solve for K_1 using

$$0 = u(d) = \int_c^d \frac{\int_c^y \frac{-2}{\sigma^2} M(r)dr + K_1}{M(y)} \mathrm{d}y. \tag{22}$$

Lacking closed form solutions to these integrals, we rely on numerical integration techniques to determine the shape of our solution $u(x)$, a function of initial position. We find that the expected exit curves of the double well

and the triple well have similar shapes when escaping from an interval whose endpoints are attracting equilibria. Expected exit time is highest at zero and gradually descends until it reaches zero at the interval endpoints. In the double well case this is the shape that we expect. Because the interval endpoints are attracting equilibria, the dynamics of the deterministic system naturally pull a particle moving along the potential into the closest well. The closer the initial position is to the well, the more quickly it exits the interval. In the triple well case we observe a plateau stretching over the x values that correspond to the intermediate well. The shape of u_{triple}, the expected exit curve associated with the triple well, demonstrates the dominance of deterministic dynamics for initial positions within the wells whose stable attractors are placed at the interval's boundary. Within the well centered at zero transitions are the result of noise and therefore the expected time to exit for processes starting within the middle well are much longer.

Lemma: Solutions $u(x)$ to the Feynman Kac formula have one and only one maximum.

Proof: Let $u(x)$ be a solution to

$$(\mathbf{L}u)(x) = b(x)u'(x) + \frac{1}{2}\sigma^2 u''(x) = -1, \quad u(c) = u(d) = 0$$

We note that since $u(x) = E_x(\tau)$ and $u(c) = u(d) = 0$, maxima do not occur on the boundary. If x is an interior maximum, $u'(x) = 0$. The fact that $(\mathbf{L}u)(x) = -1$ implies

$$-1 = \frac{1}{2}\sigma^2 u''(x)$$

and thus

$$u''(x) = \frac{-2}{\sigma^2},$$

yielding an expression of the concavity of $u(x)$.
Case 1: $u(x)$ is maximized on an interval, and $u'(x) = 0$ on some subinterval. In this case $u''(x) = 0$ on a further subinterval of $[c, d]$. However $u''(x) = \frac{-2}{\sigma^2} < 0$ at any point where u' vanishes, a contradiction.
Case 2: $u(x)$ has multiple distinct maxima. Let x_1, x_2 be points at which $u(x)$ achieves a maximum. We consider $u(x)$ on the interval $[x_1, x_2]$. We know $u(x)$ is continuous on the interval, and x_1 and x_2 are not minima. Therefore, $u(x)$ must achieve a minimum at some interior point $x_m \in (x_1, x_2)$. We conclude that $u'(x_m) = 0$ and that $u''(x_m) \geq 0$. This, however, contradicts the fact that $u''(x) = \frac{-2}{\sigma^2} < 0$.

As a result we conclude that $u(x)$ has one and only one maximum.

We first test the role of the amplitude parameter a by comparing analytical solutions for a double well and a double well with halved amplitude. Though diminished amplitude produced notable effects on expected exit time, instead of decreasing $u(x)$ it increased $u(x)$. Here we must note the difference between the transitions measured in our earlier simulations and the transitions discussed analytically. In simulations transitions are one sided; an exit is measured as the time to jump for one well to the next. On the other hand, the boundary problem that we consider analytically is a two sided exit. A transition is the time to exit the given interval in either direction. It is to this difference that we attribute this counterintuitive behavior of the system for perturbed a. Because a particle traveling along the potential may exit the interval on the side of the well at which the particle's path began, increased amplitude does not impede transitions like it would if the particle had to overcome the barrier created by increased amplitude to exit the interval. Instead, a larger barrier between the two wells creates a steeper slope that sends the particle into the closest well faster than the more moderate incline associated with a smaller barrier.

To better understand the role of a in our simulations we craft a triple well potential whose intermediate well's depth is a small fraction of that of the wells at 1 and -1. In this case the particle will indeed cross a barrier to exit the specified interval. As a comparison we perform the same analysis on a triple well potential whose wells are all equal in depth. The results reveal the influence of both a and b. Indeed, the expected exit time for the shallow triple well is closer in shape and in magnitude to $u_{double}(x)$ than $u_{triple}(x)$, confirming our intuition that larger barriers impede transitions. Further, we are forced to reject the notion that additional wells play no role in transitions between equilibria. The expected exit time for all points along the triple well is greater than that of a double well. Instead, we hypothesize that the indifference of our earlier simulations to additional wells is a result of the interplay between amplitude and intermediate wells. The additional wells in our simulations were never as deep as the wells of the corresponding double well. We suggest that the effect of the additional wells is lessened by their relative shallowness. We posit that in our simulative setting additional wells steepen the slopes between wells, decreasing the transition time governed by deterministic dynamics and further offsetting the effects of additional wells.

To glean a better understanding of the stochastic dynamics of the double and triple well systems we consider analytical solutions to the same problem for boundary points that are not centered at attracting equilibria. Because the boundary points are centered at the minima the exits discussed above are driven by deterministic dynamics. The graphs below are solutions to the

expected exit time from the interval $(-1.2, 1.2)$. The value of the potential at the boundary is no longer a minimum, exits are a result of noise. From these solutions we observe the effect of deterministic perturbations on the stochastic dynamics of the system. The shape of the expected exit curves are comparable to the expected exit curves for the interval $(-1, 1)$, suggesting the observed influence of parameters a and b hold in the larger simulative context in which a particle must transition between many equilibria to successfully exit. In particular, the relative dominance of the parameters a and b remains consistent as demonstrated by figures 6-8.

The relative strength of the deterministic and stochastic dynamics is further illustrated by the results of changes in σ. Figure 9 shows the expected exit time from the interval $(-1.2, 1.2)$ for a double well potential subjected to noise with halved magnitude. The expected exit curve dominates $u_{double}(x)$ for all initial values within the interval. From this we confirm that noise levels play a notable role in determining expected transition time.

Our analytical results suggest that the phenomena observed during simulations is a product of interplay between parameters. The role of a and b depends on the dominance of stochastic dynamics. In this case amplitude plays a significant role just as we saw during simulations. The effect of additional wells is likely offset by their relatively small amplitude. While simulations suggested that the number of additional wells was irrelevant in the calculation of expected transition time, they failed to reveal the interaction between parameters. We conclude that in this moderate noise regime our counterintuitive simulative observations are a result of more than randomness.

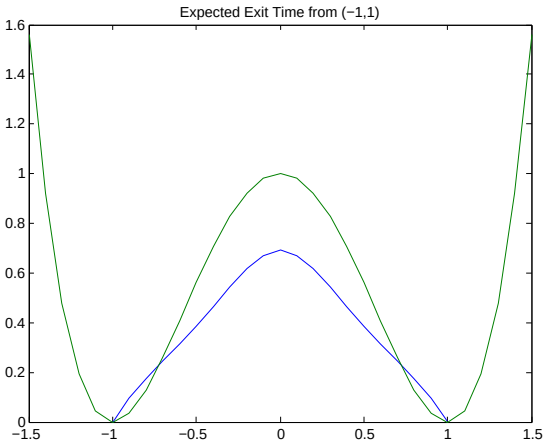

Figure 2: Double well exits from (-1,1)

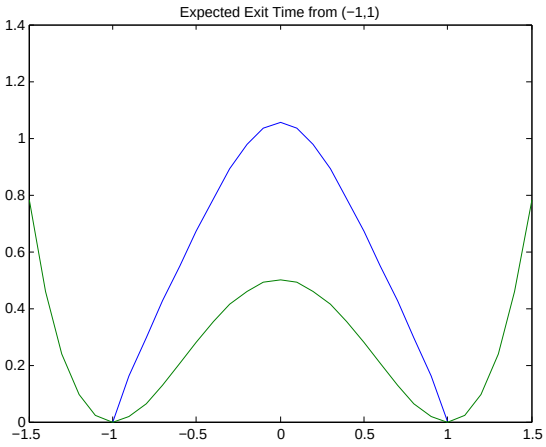

Figure 3: Double well with halved a exits from (-1,1)

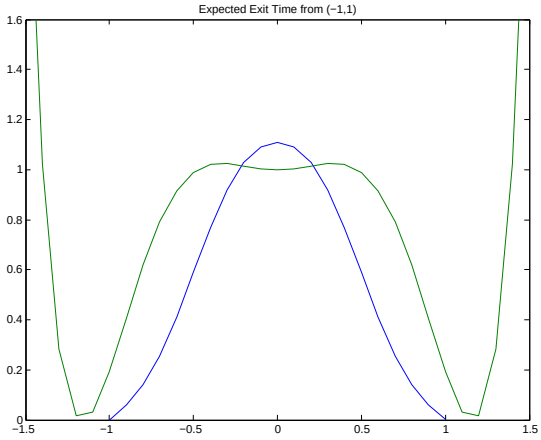

Figure 4: Triple well with shallow intermediate well exits from (-1,1)

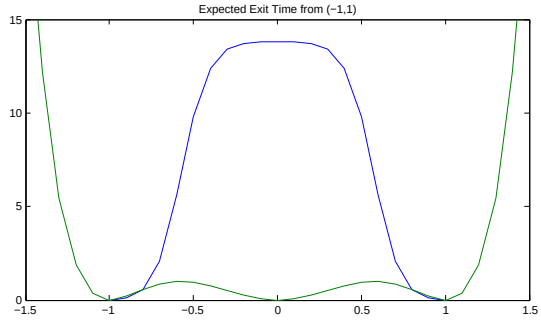

Figure 5: Triple well exits from (-1,1)

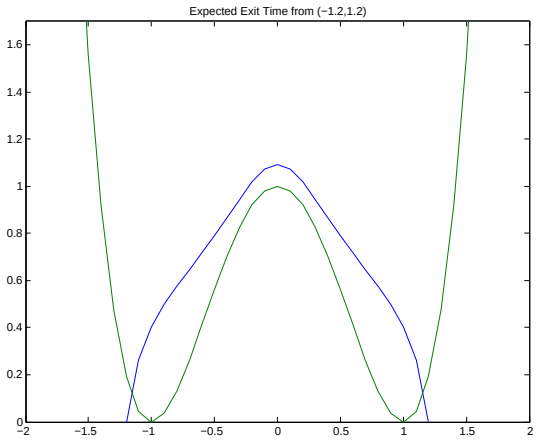

Figure 6: Double well exits from (-1.2,1.2)

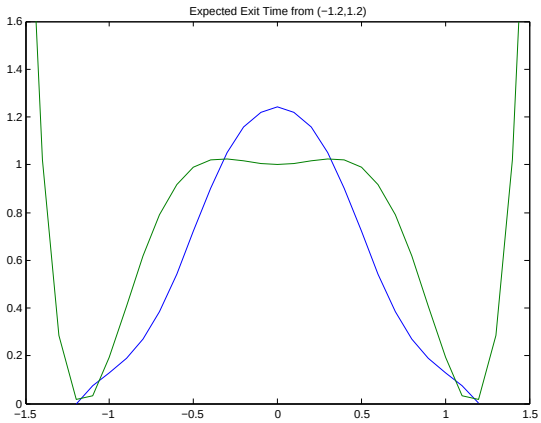

Figure 7: Triple well with shallow intermediate well exits from (-1.2,1.2)

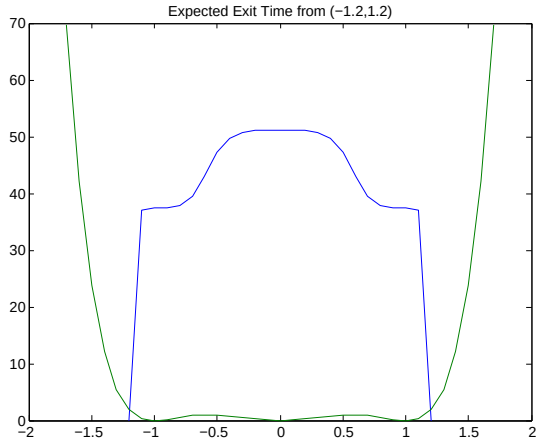

Figure 8: Triple well exits from (-1.2,1.2)

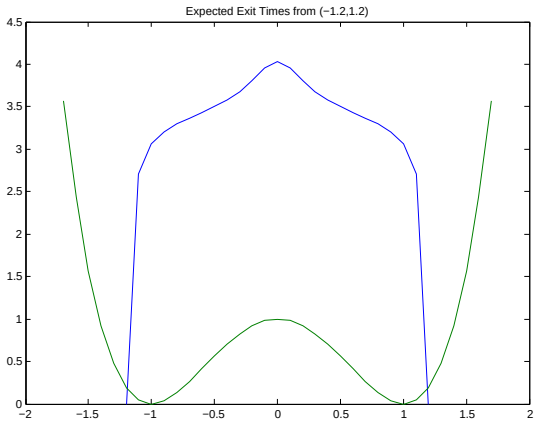

Figure 9: Double well with halved noise strength exits from (-1.2,1.2)

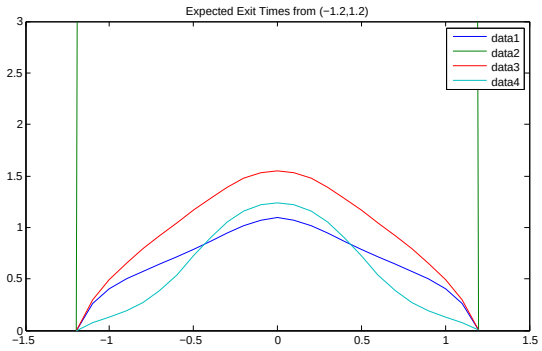

Figure 10: A comparison of u(x) for double (blue), triple (green), shallow double (red), and shallow triple (teal) potentials

.

4 Breathing Potential

The second system we will discuss we call the breathing potential. This system received its name from its sinusoidal time component which causes periodic shifts over time. A simplification of the Morris Lecar model of neural stimulation, the breathing potential represents another modeling application of noise induced transitions.

Neuron activation is the result an electrical current down the cell's plasma membrane. This change in potential opens voltage gated ion channels, which allows positively charged sodium and calcium ions to flow across the membrane into the cell. Once the current has passed, the gates close, trapping the foreign ions and changing the polarity of the membrane. This causes potassium channels to open to allow the flow of potassium ions out of the cell membrane to restore balance.

There are a number of models of neuron activation, the most precise of which is the Hodgkin Huxley model. The HH equations derive their accuracy from a complex system of nonlinear differential equations. We, however are interested in a simplifying the model to better understand the processes driving neural excitation. For this we turn to the Morris Lecar model. In their study of the effects of current stimulation in a barnacle muscle fibers Drs. Morris and Lecar observed a number of oscillatory behaviors in the measured voltage across the muscle. Instead of relying on the more complicated Hodgkin-Huxley model of neural excitation, Morris and Lecar developed a simpler model of two non-inactivating conductance to model the behavior they observed.

The Morris Lecar model is a two dimensional model which depends on the voltage of the stimulus, $V(t)$, and a recovery variable $W(t)$, which represents the reactive flow of potassium ions. Morris and Lecar's equation may be represented as follows:

$$C\frac{\mathrm{d}V}{\mathrm{d}t} = -I_{ion}(V,W) + I \tag{23}$$

$$\frac{\mathrm{d}W}{\mathrm{d}t} = \phi\frac{[W_\infty(V) - W]}{\tau_W(V)} \tag{24}$$

where

$$I_{ion}(V,W) = g_{Ca}m_\infty(V)(V - V_{Ca}) + g_K W(V - V_K) + g_L(V - V_L), \tag{25}$$

g_i represents the total conductance through i-type channels, ϕ is a scaled temperature, and m and τ are V dependent functions [8] . The behavior

of the model is characterized by its equilibria. To find these we consider the phase plane portrait of the system and the V and W nullclines, where $\frac{dV}{dt} = 0$ and $\frac{dW}{dt} = 0$. At the intersection of the nullclines is a attracting point equilibrium. Variation of the parameter I determines the additional equilibria demonstrated by a model. For many values of I, the system exhibits both a stable steady state at a fixed point and a stable limit cycle. These attracting equilibria are separated by an unstable limit cycle. Initial values within the unstable limit cycle tend toward the steady state, whereas initial values outside tend toward the stable limit cycle. Times when the system falls into the stable limit cycle correspond with neural repetitive firing, and example of the oscillatory voltage measurements observed by Morris and Lecar. Human cognition implies that, in the context of this model, the system quits the confines of the limit cycle frequently. This, in turn, suggests the existence of a certain amount of randomness associated with the behavior of the system. It is this noise driven behavior that our work with the breathing potential strives to understand.

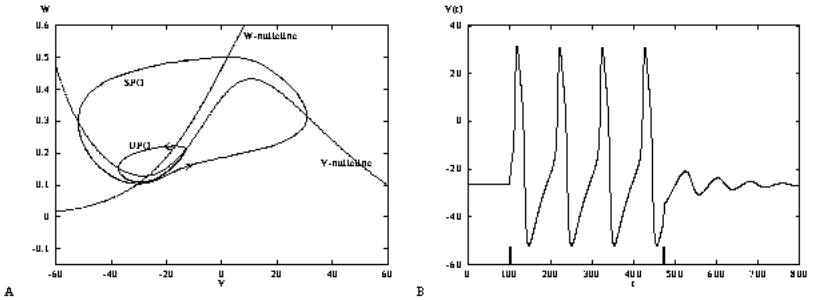

Figure 11: Left: Phase portrait and nullclines of a Morris Lecar neuron. Right: A plot of voltage spikes associated with the model's dynamics over time [4]

4.1 Building a Simpler Model

Keeping with the theme of this paper, in this section we apply our understanding of noise driven transitions to the Morris Lecar model. For values of the parameter I for which the model demonstrates bistability we can consider transitions from one attracting equilibrium to another much like we did in the double well context. In this case we will consider a single well potential whose attracting equilibrium at the bottom of its well corresponds

to the fixed point of the Morris Lecar model. Transitions out of the well are measured as the times when the system exits a given height interval along the potential curve. This approach allows us to measure the time between transition much like we did in the previous section.

The model, however, is complicated by time dependency. Prior simulations and analysis indicates that the system's inclination to cross the unstable limit cycle varies as a function of time [8]. At different points along the unstable limit cycle the model is more likely to fall into the repetitive firing behavior associated with the stable limit cycle than at other points. Because the barrier created by the unstable cycle between the attracting equilibria is a cycle, the time dependence of the model's tendency to transition is cyclical. This nonuniform inclination to transition from the stable limit cycle is the inspiration for our simulations with the one dimensional time-dependent potential mode described below.

The potential we will consider we have coined the breathing potential. The breathing potential is an extension of a single well potential model. Shaped like a parabola, a single well is a well established method of measuring the waiting time until a particle moving along the potential exceeds a certain height along the potential. Our breathing potential behaves similarly, with the addition of periodic oscillations from a positive to a negative potential. This behavior captures the periodic variability of the forces encouraging the system to transition to the stable limit cycle. In other words, at times when the model invites transitions, the breathing potential is positive. However, when the barrier to deviations from the steady state is great, the potential is negative. We define the potential to be

$$U_{breathing}(x,t) = \alpha \sin(\omega t) * x^2 \tag{26}$$

where α is the amplitude of the oscillation and ω is the period. Movement along a potential defined this way is purely deterministic and ignores transitions between equilibria. To account for these jumps we define the behavior of the model as

$$\mathrm{d}Y_t = -U'_{breathing}(x)\mathrm{d}t + \sigma \mathrm{d}W_t \tag{27}$$

where $\mathrm{d}W_t$ represents an increment of Brownian motion. We strive to understand whether the simpler breathing potential model is a reasonable alternative to the Morris Lecar model and the Hodkin-Huxley equations.

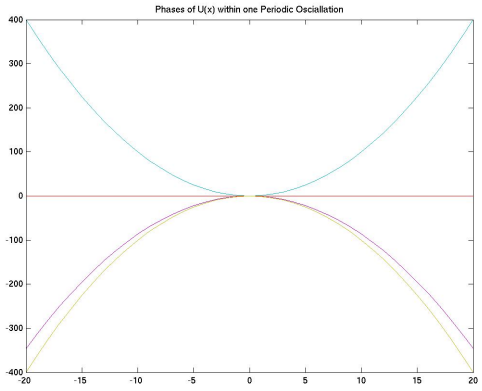

Figure 12: An example of the breathing potential at various values of t.

4.2 Simulations

Many of the methods employed in our double well endeavors were reused in the breathing potential context. We first tracked the behavior of Y_t to glean qualitative understanding of our model. After observing a number of realizations of the Y_t trajectory we were convinced that a priori the model's transitions were consistent with the behavior expected of a Morris Lecar neuron. We next asked whether transitions between equilibria occurred at times that the model designates as more conducive to transitions. To answer this query we measured the time of first exit from an interval. In this set of simulations the interval corresponds to the maximum height along the potential which represents the barrier to transitions from the stable fixed point. For the parameter values $\alpha = .1$, $\omega = 3\pi$, and $\sigma = .4$ we determined from our qualitative observations that an appropriate maximum barrier height L is 2. Having recorded the times of first exit we plotted the potential well $U_{breathing}(Y, t)$ for the measured value of t. This yields a graphical representation of the barrier to transition. We expect exits to coincide with negative or downward facing $U_{breathing}$ curves which represent times at which the model encourages transitions.

4.3 Results

Our qualitative observations indeed mirror the results expected of a Morris Lecar neuron. Periods of quiescence are followed by long periods outside of

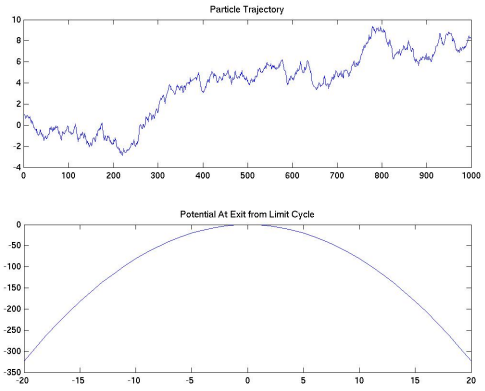

Figure 13: Above- an example X_t trajectory. Upon crossing the boundary $L = 2$ X_t remains outside of the interval for a significant duration, a phenomenon consistent with repetitive neuron firing. Below- a pictorial representation of the breathing potential at the time that X_t crossed the boundary. The potential is negative, meaning the transition occurred at a point at which the system encourages jumps.

the interval corresponding to the stable fixed point. Time spent outside of the fixed point equilibrium correspond with time spent in the excited state represented by the stable limit cycle. The more time steps spent in the stable limit cycle results in more cycles of activation and, therefore, in the repetitive firing observed by Morris and Lecar.

Further, our time of first exit simulations support the validity of the breathing potential model. Times spent outside of the interval quiescence begin at times when the deterministic breathing potential $U_{breathing}(x,t)$ is negative. We infer that the oscillating time component of the breathing potential accurately captures the variability of the barrier to transition from one stable equilibrium to another given α, ω, and σ.

5 Conclusion

In a world filled with uncertainty, realistic models must incorporate an element of randomness. In our paper we examine two such models: the double well potential system and the Morris Lecar model of neuron activation. In particular, we explore the effects of deterministic perturbations on transi-

tions between stable equilibria in stochastic dynamical systems. The first section is dedicated to the study of perturbations without time dependence in double well potential variations. The second section focuses on a biological manifestation of transitions between stable equilibria, the model of which relies on time dependent parameters. We find that in moderate noise regimes the interaction between parameters produces results we would not expect from perturbations of a single parameter.

In both of the cases discussed in this paper we choose σ so be a fixed moderate noise strength. This facilitates simulations by driving transitions on reasonable time frames. It would be interesting, however, to study the effects of decreasing σ. The theory of large deviations provides a framework for thinking about such small noise limits. An extension of this work might consider the effects of deterministic perturbations in the small noise setting to determine whether interactions between parameters play the same role in the behavior of rare transitions.

6 Acknowledgements

Many thanks to Dr. Avanti Athreya, Dr. David Kraines, and Dr. Jonathan Mattingly for sponsoring this project through the PRUV program, and also to Dr. Jordan Eccles for his ever available simulative genius.

References

[1] Anderson, David and Jonathan Mattingly. (2011) *A Weak Trapezoidal Method for a Class of Stochastic Differential Equations.* Commun. Math. Sci. Vol 9, No. 1, pgs 301-318.

[2] Bhattacharya, Rabi and Edward Waymire. (2009) *Stochastic Processes with Applications.* New York: SIAM.

[3] Durrett, Rick. (2010) *Essentials of Stochastic Processes.*New York: Springer.

[4] Ermentrout, G.B. and J. Rinzel. (July 29, 1996) *Analysis of Neural Excitability.* Retrieved from http://www.math.pitt.edu/ bard/bardware/meth3/node3.html.

[5] Freidlin M., Wentzell, A. (1998) *Random Perturbations of Dynamical Systems* New York: Springer.

[6] Karatzas, Ioannis, and Steven E. Shreve. (1988) *Brownian MOtion and Stochastic Calculus*. New York: Springer.

[7] Lawler, Gregory. (2006) *Introduction to Stochastic Processes*. Boca Raton: Chapman & Hall/CRC.

[8] Morris, Catherine and Harold Lecar. (1981) *Voltage Oscillations in the Barnacle Giant Muscle Fiber*. Biophysical Journal. Vol 35, pgs 193-213.

[9] Oksendal, Bernt. (2003) *Stochastic Differential Equations: An Introduction with Applications*. New York: Springer.